PCCP

PAPER

View Article Online
View Journal | View Issue

Cite this: *Phys. Chem. Chem. Phys.*, 2019, **21**, 3512

On the simulation of vibrationally resolved electronic spectra of medium-size molecules: the case of styryl substituted BODIPYs†

Mariagrazia Fortino,[a] Julien Bloino,*[bc] Elisabetta Collini,[d] Luca Bolzonello,[d] Mariachiara Trapani,[e] Francesco Faglioni[a] and Alfonso Pedone*[a]

Received 4th May 2018,
Accepted 18th July 2018

DOI: 10.1039/c8cp02845a

rsc.li/pccp

BODIPY dyes are used in a variety of applications because of their peculiar spectroscopic and photophysical properties that vary depending on the stereochemistry of the functional groups attached to the boron-dipyrromethene core structure. In this work, we have applied several computational methods, adapted for semi-rigid molecules based on the Franck–Condon principle, for the study of the optical properties of BODIPY systems and for the understanding of the influence of functional groups on their spectroscopic features. We have analyzed the electronic spectra of two styryl substituted BODIPY molecules of technological interest, properly taking into account the vibronic contribution. For comparison with recently recorded experimental data in methanol, the vibrationally resolved electronic spectra of these systems were computed using both Time-Independent (TI) and Time-Dependent (TD) formalisms. The first step toward the analysis of optical properties of the styryl modified BODIPYs was a benchmark of several density functionals, to select the most appropriate one. We have found that all benchmarked functionals provide good results in terms of band shape but some of them show strong discrepancies in terms of band position. Beyond the issue of the electronic structure calculation method, different levels of sophistication can be adopted for the calculation of vibronic transitions. In this study, the effect of mode couplings and the influence of the Herzberg–Teller terms on the theoretical spectra has been investigated. It has been found that all levels of theory considered give reproducible results for the investigated systems: band positions and shapes are similar at all levels and little improvements have been found in terms of band shape with the inclusion of Herzberg–Teller effect. Inclusion of temperature effects proved to be challenging due to the important impact of large amplitude motions. Better agreement can be achieved by adopting a suitable set of coordinates coupled with a reduced-dimensionality scheme.

Introduction

Thanks to their optical properties, BODIPY dyes form a class of extremely versatile fluorophores used in several applications as chemical sensors, labeling agents, or luminescent devices.[1–4] Indeed, their large molar absorption coefficients and good fluorescence quantum yields, combined with their high thermal and chemical stabilities, make them particularly suitable for the design of dye-sensitized solar cells. Thanks to their easy functionalization, it is possible to finely tune these properties. However, the right configuration can only be found after reaching a deep understanding of the physicochemical properties of the dyes and the effect of functionalization. This task is nowadays strongly supported by computational chemistry and spectroscopy, which can also be used to predict the performance of new derivatives and identify the most interesting candidates for further studies.

Such computational studies are commonly done by means of density functional theory (DFT) and its time-dependent extension (TD-DFT),[5–15] which offer a good balance between computational cost and accuracy.

The performance of TD-DFT on the reproduction of vertical and adiabatic energies of valence transitions in several BODIPY

[a] *Università di Modena e Reggio Emilia, Modena, 41125, Italy. E-mail: alfonso.pedone@unimore.it*
[b] *Consiglio Nazionale delle Ricerche Istituto di Chimica dei Composti OrganoMetallici, Pisa, I-56124, Italy*
[c] *Scuola Normale Superiore di Pisa, Piazza dei Cavalieri 7, I-56126 Pisa, Italy. E-mail: julien.bloino@sns.it*
[d] *Università degli studi di Padova, Padova, 35131, Italy*
[e] *CNR-ISMN, Istituto per lo Studio dei Materiali Nanostrutturati, c/o Dipartimento di Scienze Chimiche, Biologiche, Farmaceutiche ed Ambientali, 98166, Messina, Italy*

† Electronic supplementary information (ESI) available. See DOI: 10.1039/c8cp02845a

derivatives has been extensively studied in the past by Jacquemin *et al.*[16–19] These investigations and others have shown that the expected TD-DFT accuracy is strongly dependent on the nature of the considered state and the functional, and that TD-DFT usually overestimates the vertical excitation energy with respect to experiments and high-level post-HF calculations.[16–23]

These discrepancies have been imputed to the double excitation contribution to the first singlet excited states of BODIPY derivatives that cannot be recovered at the TDDFT level.[22] However, despite this, several studies showed that popular hybrid functionals such as B3LYP and PBE0 provide vertical transition wavelengths in fair agreement with the maximal absorption (λ_{max}) for aza-BODIPY[16,24] and BODIPY.[25,26] The apparent accuracy can be explained by an error cancelation phenomenon between (i) the neglect of vibrational (and often solvation) effects and (ii) the inherent inaccuracy of TD-DFT for describing transition energies to states involving a significant double character.

The choice of the most reliable method is often done by simulating the UV-vis spectra based on pure electronic transitions, which are subsequently broadened to match the experimental band-shape and compare the absorption and emission wavelengths. However, such an approach completely ignores the vibrational structure present even in low-resolution spectra, and responsible for the asymmetry of band-shapes. A direct consequence of this approximation is the risk of incorrectly evaluating the maxima positions, which may result in a wrong assessment of the accuracy of each functional. For a more accurate representation of UV-vis absorption and emission spectra, a proper account of the vibrational structure is necessary.[27–31] Compared to vertical excitation (VE) calculations, this requires the potential energy surface (PES) of each electronic state involved in the transition. As a result, the overall computational cost can be significantly higher. Nevertheless, thanks to the availability of analytic harmonic force constants even for TD-DFT,[32–34] this approach remains feasible even for molecular systems of dozens of atoms. These vibrationally resolved electronic spectra, also called vibronic spectra, depend primarily on multiple parameters: (1) the excitation energy and electronic transition moment, and (2) the shape of the initial and final PESs. The former group determines the absolute position of the band-shape and the intensity of the electronic transition, while the latter influences the magnitude of the overlap integrals and thus the band-shape. Hence, the quality of each functional must be evaluated with respect to each of these criteria. In a sum-over-states formalism, the overall band-shape is obtained as the superposition of individual transitions between the vibrational levels belonging to different electronic states. This way, it is also possible to analyze the importance of the temperature on the experimental band-shape, and the origin and nature of the observed changes. A known challenge of this method is to keep the computational cost acceptable, which means being able to identify and treat only the transitions actually contributing significantly to the band-shape. Prescreening methods can be used for this purpose, but are often insufficient in the presence of temperature effects. In these conditions, a more suitable way to simulate the vibronic spectra is offered by the path integral formalism in which the band-shape is obtained as the Fourier transform of an autocorrelation function calculated within the time domain. An interesting feature of this method is to automatically include all initial and final vibrational states, leading to accurate band-shapes at any temperature with no additional computational cost. By definition, however, it is not possible to know the contributions of individual vibronic transitions. For this reason, the two formalisms are complementary; the path integral (or time-dependent formulation, TD[35]) provides full band-shapes, while the sum over states (or time-independent, TI[36]) can be used to analyze the contributions of one or more transitions within the whole band-shape.[37–39]

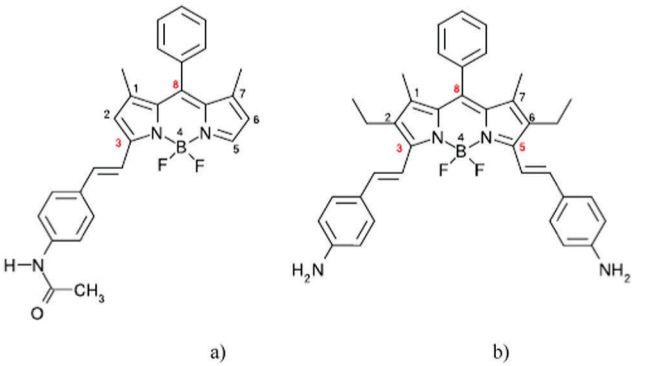

Fig. 1 (a) 8-Phenyl-3-amidestyryl-1,7-dimethyl-bodipy(**mono-bdp**) (b) 8-phenyl-3,5-di(diamino)styryl-1,7-dimethyl-2,6-diethyl-bodipy (**bis-bdp**).

In this work, we show how methods based on the Franck–Condon principle, well adapted for semi-rigid molecules, can be applied to the study of optical properties of BODIPY dyes and the influence of functional groups on their spectroscopic features, especially absorption and emission wavelengths and charge transfer. Often the information contained in the recorded spectra can be difficult to explain in a phenomenological way and appropriate theoretical models can be excellent tools to understand the peculiarities observed in the band-shape of the spectra and other properties.

To this end, we have investigated the vibrationally resolved electronic spectra of two synthesized styryl substituted boron-dipyrromethene (BODIPY) molecules of technological interest: the 8-phenyl-3-amidestyryl-1,7-dimethyl-bodipy and the 8-phenyl-3,5-di(diamino)styryl-1,7-dimethyl-2,6-diethyl-bodipy, reported in Fig. 1 and recently spectroscopically characterized.[40] We will refer to these molecules as **mono-bdp** and **bis-bdp**, respectively. Considering the flexibility of the ethyl groups in positions 2 and 6, compared to their extremely limited impact on the overall spectroscopic properties, the latter system has been modified with respect to the experimental one by replacing these chains with hydrogens. For comparison with the available experimental counterparts recorded in methanol, the vibronic spectra of the two substituted BODIPYs have been computed using both TI and TD formalisms.

As remarked above, given the great multitude of available exchange–correlation functionals, it is essential to make an accurate and careful selection of the most appropriate one for

the system and properties of interest. Several past investigations have shown that range-corrected hybrid functionals (that use fractions of exact exchange decreasing with the interelectronic distance) give good results regarding both absorption/emission energies and band-shape.[19,29,41–43] As a first step toward the analysis of spectroscopic properties of styryl substituted boron-dipyrromethenes, several popular exchange–correlation functionals have been benchmarked. This selection process will then serve as a basis for a deeper analysis of the absorption and emission spectra of **mono-bdp** and **bis-bdp**.

Methods

Computational strategies for vibrationally resolved electronic spectra

For a better understanding of the computational strategies available for simulations of vibrationally resolved electronic spectra, a short introduction to the main theoretical and technical aspects is provided. A more extensive presentation can be found in ref. 38, 39 and 44.

The spectral band-shape is seen as a superposition of individual transitions between vibrational levels belonging to different electronic states. For one-photon absorption (OPA) and emission (OPE) spectroscopies, only two electronic states are involved and the absorbed or emitted intensity can be written as,

$$I(\omega_0) = \alpha\omega_0^{\beta} \sum_{\mathrm{I,F}} \rho_{\mathrm{I}} \left|\left\langle \psi_{\mathrm{I}}^{\mathrm{v}} \middle| \boldsymbol{\mu}^{\mathrm{e}} \middle| \psi_{\mathrm{F}}^{\mathrm{v}} \right\rangle\right|^2 \delta(\Delta E + |\varepsilon_{\mathrm{F}} - \varepsilon_{\mathrm{I}}| - \omega_0) \quad (1)$$

where ω_0 is the incident or emitted energy, ΔE is the energy difference between the PESs minima, and ε_{I} and ε_{F} are the energies of the vibrational states, all expressed in wave numbers. α and β are quantities dependent on the type of spectroscopy, with α being a constant factor and β an exponent (1 for OPA, 4 for OPE). In practice, the Dirac function is replaced by a distribution function to simulate the broadening observed experimentally. It is important to note that the summation over the initial (I) and final (F) vibrational states is theoretically infinite. In the absence of temperature effects, only the initial vibrational ground state is populated so that the sum over I can be removed. For the final state, a truncation is necessary. Since only a finite number of transitions contribute in a significant way to the band-shape, it is thus possible to limit the computational cost without affecting the accuracy of the simulations, provided a way can be found to guess which transitions will be relevant. Here, a class-based prescreening is adopted, which relies on the probability of transitions of overtones and combinations of two modes to predict the most important terms in the summation (more details can be found in ref. 44 and 45).

Setting aside the problem of the summation, the main hurdle to the calculation of $I(\omega_0)$ is the evaluation of the overlap integral $|\langle\psi_{\mathrm{I}}^{\mathrm{v}}|\boldsymbol{\mu}^{\mathrm{e}}|\psi_{\mathrm{F}}^{\mathrm{v}}\rangle|$, directly related to the dependence of the electronic transition dipole moment on the nuclear coordinates and the definition of the vibrational wave function ψ^{v}. Within the Franck–Condon principle, the former is assumed to be constant. While this approximation is generally satisfactory for fully-allowed transitions, it can be insufficient otherwise. Herzberg and Teller proposed a refinement by assuming a linear dependence of $\boldsymbol{\mu}^{\mathrm{e}}$ with respect to the normal coordinates of vibrations $\mathbf{Q}$.[46] More generally, $\boldsymbol{\mu}^{\mathrm{e}}$ is expanded in a Taylor series with respect to the normal coordinates about the equilibrium geometry of one of the electronic states, with the zeroth-order (constant) term corresponding to the Franck–Condon (FC) approximation and the first-order term to the Herzberg–Teller (HT) approximation. The combination of the two terms will be referred to as FCHT in the following for clarity. For the definition of the vibrational wavefunction, except for very specific cases involving small or rigid and symmetric molecules, the number of relevant transitions to account for the simulation of the overall band-shape is generally high, so the anharmonic approximation is too expensive to be tractable. As a result, ψ^{v} is assumed harmonic, and the associated vibrational state will be noted in the following as a vector of harmonic quanta, $|\nu\rangle$. Even in this case, a problem persists for the calculation of the integral since the wave functions are expressed in different basis sets (one per electronic state). This can be solved by defining a relation between the two sets of normal coordinates, usually the linear transformation proposed by Duschinsky,

$$\mathbf{Q}_{\mathrm{I}} = \mathbf{J}\mathbf{Q}_{\mathrm{F}} + \mathbf{K}$$

when temperature effects are important, the performance of the sum-over-states approach worsens since the number of initial states to consider can become very large and efficient prescreening procedures are no longer sufficient, especially for large systems. The path integral or time-dependent (TD) formulation can then be used to overcome this problem. The idea is first to replace the Dirac function in eqn (1) with its Fourier transform[35] and switch to the time domain. The total intensity can then be rewritten as follows:

$$I(\omega_0) = \alpha'\omega_0^{\beta} \int_{-\infty}^{+\infty} \mathrm{d}t\, \mathrm{Tr}\left(\boldsymbol{\mu}^{\mathrm{e}} \mathrm{e}^{-\tau_{\mathrm{F}} H_{\mathrm{F}}} \boldsymbol{\mu}^{\mathrm{e}} \mathrm{e}^{-\tau_{\mathrm{I}} H_{\mathrm{I}}}\right) \mathrm{e}^{i2\pi c(\Delta E - \omega_0)t} \quad (2)$$

where $\mathrm{Tr}(\boldsymbol{\mu}^{\mathrm{e}}\mathrm{e}^{-\tau_{\mathrm{F}}H_{\mathrm{F}}}\boldsymbol{\mu}^{\mathrm{e}}\mathrm{e}^{-\tau_{\mathrm{I}}H_{\mathrm{I}}})$ is the electronic transition dipole moment autocorrelation function. τ_{I} and τ_{F} are complex variables that depend on simulation time and temperature and H_{I} and H_{F} are vibrational Hamiltonians of the initial and final electronic states. A particularly interesting property is that the TD approach includes implicitly all initial and final vibronic states, so the computational cost does not depend on temperature. However, a consequence of this is the loss of information about the contributions of each transition to the overall band-shape. For this reason, the sum-over-states (TI) and TD approaches are complementary for one-photon spectroscopies. The TD procedure gives converged band-shapes and a good estimate of temperature effects, while TI allows having information about individual contributions of each transitions to the band-shape, giving an insight into its fine structure.[39,41,44]

If the PES minima are not superimposed, which means that structural relaxation occurs upon the electronic transition, the harmonic approximation, in particular for the final state, can have a significant impact on simulation accuracy. In such cases, two choices can be made regarding the calculation of the

final-state harmonic PES depending on which aspect of the band-shape is more important. If a correct evaluation of the most intense transitions is critical, the initial-state equilibrium geometry should be used as a reference for the calculation of the final-state PES, which corresponds to the so-called vertical Hessian approach (VH). Otherwise, the adiabatic Hessian (AH) approach, where the PES is calculated about its own minimum, provides a more balanced picture, in particular regarding the transition energies. Another important aspect of VH is that, since the PES is calculated outside its minimum, the method is more sensitive to the anharmonicity, so AH is often preferred by default. Nevertheless, for small changes, AH and VH are expected to give almost equivalent results. Even with the availability of analytic force constants for ground- and excited-states, this step still represents a significant cost. Cheaper variants, named adiabatic shift (AS) and vertical gradient (VG) assume that the final-state PES is the same as the initial one, so only one frequency calculation is needed, removing the mode mixing expected with the transition. These approximations are generally relevant for absorption processes since computing excited-state PESs is more expensive than for the ground state, especially if analytic formulas are not available.[39,45,47–49] Here, adiabatic approaches will be employed.

Computational details

All DFT and TD-DFT calculations have been performed with a locally modified version of the Gaussian16 suite of quantum chemical programs.[50] The Adiabatic Hessian model has been used for most vibronic calculations. Hence, we performed a geometry optimization followed by frequency calculations for both ground and excited states. For this reason, the first step of our investigation has been to compute the ground- and excited-state minima and frequencies necessary to generate the vibronic spectra of **mono-bdp** and **bis-bdp** using several exchange–correlation functionals.

We used hybrid functionals, namely B3LYP and PBE0, long-range corrected functionals, such as CAM-B3LYP and ωB97X, and Minnesota functionals, namely M06-2X and MN15.[51–56] In the investigations performed using B3LYP, PBE0 and CAM-B3LYP, Grimme's empirical D3 dispersion corrections have been included, while for ωB97X, Grimme's empirical D2 dispersion corrections have been used.[57–59] Cartesian coordinates for the optimized structures of **mono-bdp** and **bis-bdp** systems with the MN15 functional, both in the ground and excited states, are reported in the ESI.†

In all calculations, we have employed the 6-311G(d,p) basis set. To probe the effect of diffuse functions, some computations were also performed with the 6-311+G(d,p) basis set. Comparing vertical excitation energies and the electronic transition dipole moment obtained with the two basis sets, we have found no significant differences and thus, considering the higher computational cost associated with diffuse functions, we have chosen to use 6-311G(d,p) (see Table S1 in ESI†). The effect of methanol as solvent has been taken into account by using the integral equation formalism for the polarizable continuum model (IEF-PCM, referred to simply as PCM in the following).[60] The default parameters of Gaussian16 have been used for the construction of the cavity, built as the envelope of interlocked spheres centered on each atom of the solute. For the investigation of the absorption and emission processes, two approaches are usually employed: the conventional linear-response (LR) and the state-specific (SS) approaches.[61,62] In the SS approach the solvent reaction field is computed self-consistently using the electron density of the state of interest, while in the LR method the absorption and emission energies are determined including a PCM correction dependent on the electron density variation associated with the transition. Moreover, in the PCM approach, two limit time regimes can be chosen to express the solute–solvent interaction, the equilibrium (EQ) and the non-equilibrium (NEQ) regime. In the EQ regime, all electronic and nuclear solvent degrees of freedom are in equilibrium with the electron density of the solute, whereas in the NEQ regime only the solvent electronic polarization is in equilibrium with the excited-state electron density. Past investigations have shown that NEQ-PCM model is more suitable for electronic calculations of absorption processes in solution, while EQ-PCM is the preferred choice for the study of excited-state structural relaxation processes.[63] In this work, the vertical excitation and emission energies of the two molecules in methanol have been computed employing the NEQ-LR-PCM and EQ-SS-PCM approaches, respectively.

Regarding the vibronic calculation, both TI and TD approaches have been used, especially at the adiabatic Hessian (AH) level of theory but some investigations have also been performed with the adiabatic shift (AS) approximation. In the following, the vibronic model used for the simulation of the spectra will be specified by combining the framework (TI or TD), and the model used for the representation of the potential energy surfaces (AS or AH) together with the electronic transition moment (FC or FCHT). For instance, TI AH|FCHT will refer to the sum-over-states formulation coupled with the AH model and the electronic transition dipole moment expanded as a Taylor series up to the first-order included. It is noteworthy that for the adiabatic models (AH and AS) the EQ-SS-PCM is always used, for both emission and absorption spectra. Within the TD framework, temperature effects have been automatically included without additional computational cost. For this reason, in the TD framework the vibronic spectra have been simulated both at T = 0 K and at T = 298.15 K. For TI, the following parameters were used for the prescreening: $C_1^{\max} = 30$, $C_2^{\max} = 25$, $N_I^{\max} = 10^9$ (see ref. 29 and 38). For TD, a total time of 10^{-10} s divided into 2^{24} steps was chosen.

To remove the large amplitude motions (LAMs) in the simulations accounting for temperature effects, a reduced-dimensionality (RD) scheme was employed, where all modes with wavenumbers below 50 cm^{-1} were automatically excluded. The principle is to use the Duschinsky matrix, which represents the mode mixing occurring upon the transition, to select two consistent sets of normal modes, one per electronic state. The square elements of the Duschinsky matrix (J_{ik}^2) are used to find the largest projection of each mode onto the basis of normal modes of the other electronic state. Except in very specific cases

of rigid systems where the mixing of the normal modes is negligible, most modes do not have a one-to-one correspondence with the other electronic state and a threshold needs to be set to truncate the projection. The elements J_{ik}^2 are then sorted by decreasing magnitude along a given row (when choosing the projection of an initial-state mode) or column (for the final state) and a number of elements is selected until a given percentage of the total sum along the row or column is selected. By doing this iteratively as described in ref. 37 to blocks are obtained: one corresponding to the modes to remove and their counterpart or a combination of those in the other electronic state, and the remaining mode. Ideally, the discarded couplings (which would be the off-blocks terms connecting the two blocks) should be negligible. However, this may prove to be difficult for more flexible and larger molecules like the BODIPYs. For this reason, in this work, we have considered uncoupled the LAM with highest overlap above 60%. Moreover, in order to minimize the couplings, internal coordinates were used, starting from primitive internal coordinates generated from the molecular topology. The Wilson B matrix was then computed from analytic expressions of bond lengths, and valence, dihedral, and out-of-planes angles. The non-redundant, delocalized internal coordinates were obtained by means of a single value decomposition of the B matrix, using a threshold of 10^{-5} to select the singular vectors with non-negligible singular values as described in ref. 64.

Experimental details

Mono-bdp and **bis-bdp** have been synthesized following the procedure already described in ref. 65. The sample solutions were prepared by dissolving the dyes in methanol with a concentration suitable for the different spectroscopic analyses, in the order of 5–10 μM.

One-photon absorption (OPA) and one-photon emission (OPE) properties have been investigated by excitation and emission fluorescence spectroscopy, respectively. The sample was held in a 5 mm diameter capillary directly inserted in a liquid nitrogen cryostat mounted on a Horiba Jobyn Yvon Fluoromax 3. In the case of dilute solutions, the fluorescence excitation spectrum brings the same information of the absorption

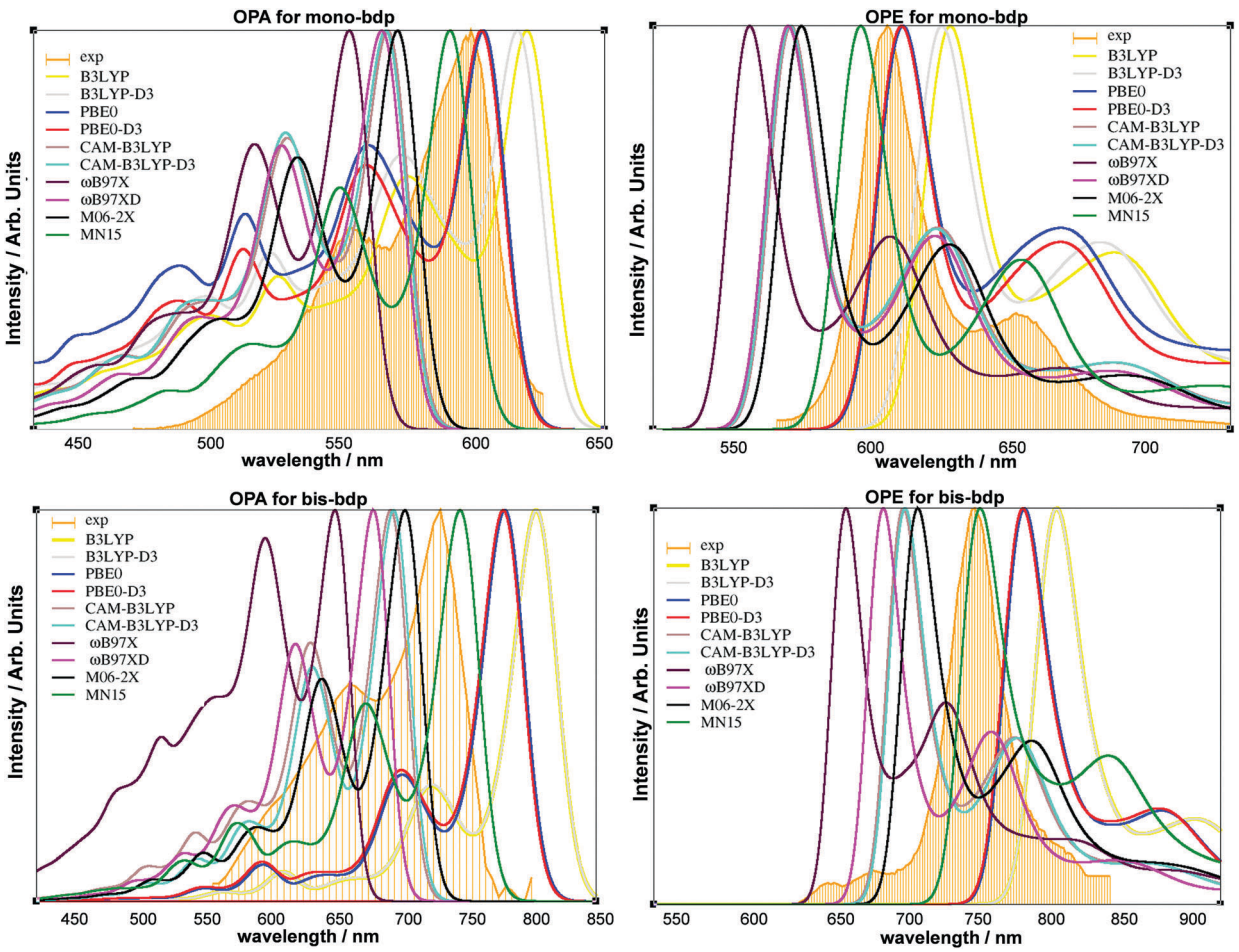

Fig. 2 Comparison of the vibronic absorption and emission spectra of **mono-bdp** and **bis-bdp** systems, computed with different exchange–correlation functionals and neglecting temperature effects, along with the experimental ones recorded at 77 K in methanol. All vibronic calculations have been performed at the TD AH|FCHT level of theory, and Gaussian distribution functions with HWHM = 250 cm^{-1} have been used to simulate the broadening.

spectrum, as confirmed in Fig. S1 of the ESI.† For this reason, in the following the fluorescence excitation spectra will be treated as experimental OPA spectra in the comparison with the simulated results. The advantage of using the fluorescence excitation spectra rather than the absorption spectrum is that it allows the comparison of OPA and OPE properties recorded in the same experimental configuration and with the same instrumentation.

Results and discussion

Vibrationally resolved electronic spectra: benchmark of exchange–correlation functionals

As discussed above, given the vast multitude of available density functionals, the first step toward the spectroscopic analysis of the styryl modified systems is a benchmark of several exchange–correlation functionals, to select the most appropriate one. Because of the huge number of functionals currently available, the benchmark was intentionally limited to a subset of well-known candidates, which have already been successfully applied to the same type of simulations on similar organic systems.[16,19,22,27,29,30,37]

In Fig. 2 the absorption and emission vibronic spectra of **mono-bdp** and **bis-bdp** molecules, computed at the TD AH|FCHT level with ten different exchange–correlation functionals and neglecting temperature effects, along with the experimental ones recorded at 77 K in methanol, are reported. This setup was chosen as it provides the highest level of accuracy for our vibronic calculations, without the risk of inaccuracies due to the truncation made in the TI framework. Furthermore, neglecting temperature effects makes the analysis of the band-shape easier and more reliable in the first benchmark step.

Both absorption and emission experimental spectra of the two modified BODIPYs present the typical shape found for organic chromophores in solution with a main peak followed by a vibronic sideband.[17] However, for the emission spectrum of the **bis-bdp** system, this feature is less evident and the second peak looks like a shoulder in the tail.

For **mono-bdp**, the dominant absorption experimental band is at 595 nm and the emission at 605 nm, whereas for **bis-bdp** the most intense absorption peak is observed at 729 nm and the emission at 751 nm. For all computed spectra, we have used Gaussian distribution functions with half-widths at half-maximum of 250 cm^{-1}. For both systems, the vibronic structure is fairly well reproduced by all ten functionals, and the computed energy differences between the two peaks match the experimental values. It is worth mentioning that some variations in the intensity of the second band in the absorption vibronic spectrum of **bis-bdp** have been found with some functionals, especially M06-2X for which this band is nearly as intense as the first one. However, the more relevant differences are observed in terms of band positions.

Fig. 2 shows that MN15, PBE0 and PBE0-D3 functionals yield vibronic transition energies in closer agreement with experiments, both for absorption and emission processes (with a shift from the experimental band positions of ~10 nm).

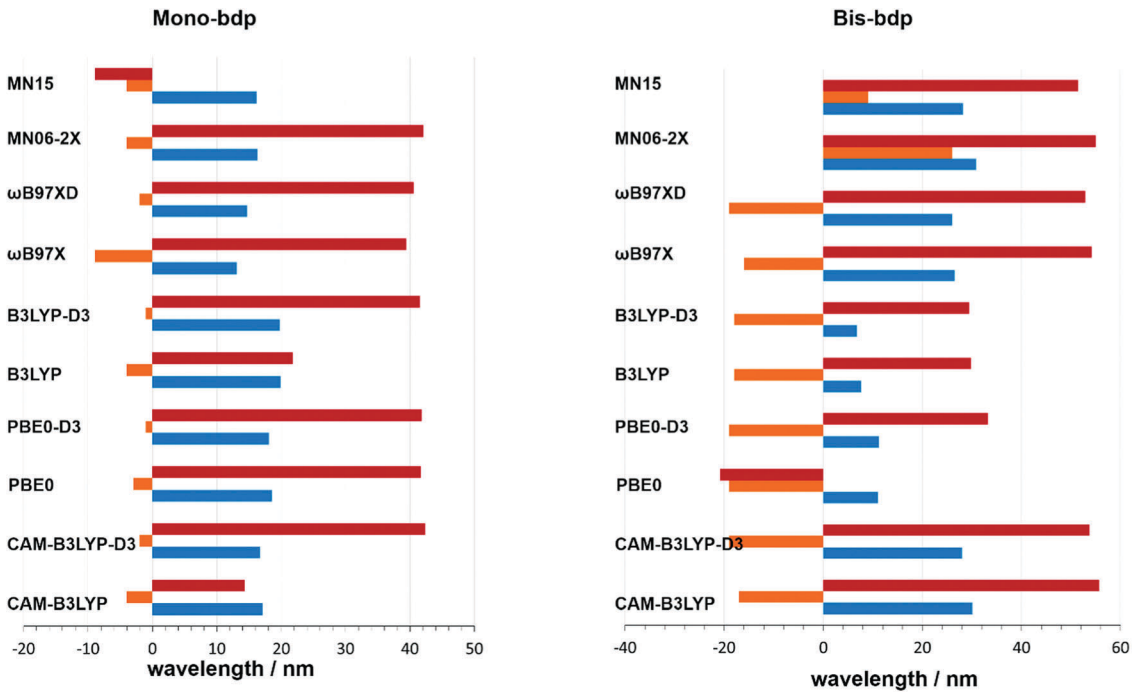

Fig. 3 Computed Stoke shift differences from experimental values with several exchange–correlation functionals obtained by using the maximum bands of the absorption and emission spectra (orange bars), the vertical excitation and emission energies computed with the NEQ-LR-PCM and EQ-SS-PCM approaches respectively (blue bars), and the vertical excitation and emission energies computed with the NEQ-SS-PCM and EQ-SS-PCM approaches, respectively (red bars). The histogram on the right collects data for **mono-bdp** and the one on the left for **bis-bdp**.

Table 1 CT distance (d_{CT}), transferred charge (q_{CT}), dipole (μ_{CT}), H and t indexes computed at the MN15/6-311G(d,p) level in methanol upon electronic excitation. These parameters have been computed using the Mulliken ground- and excited-state atomic charges, computed at the S_0 optimized geometry

	Mono-bdp	Bis-bdp
q_{CT} (e)	0.23	0.30
d_{CT} (Å)	2.24	3.21
μ_{CT} (D)	2.47	4.70
H index (Å)	2.32	2.67
t index (Å)	−0.09	0.54

Good results have also been found with M06-2X, B3LYP and B3LYP-D3 (∼20 nm), while ωB97X, ωB97X-D, CAM-B3LYP and CAM-B3LYP-D3 exchange–correlation functionals are those, which showed larger discrepancies (∼30–45 nm). For a more qualitative comparison, the effective perceived colors for a saturated solution (highest absorbance or emission peak set to 1) have been computed in the RGB space using the VMS draw program[66] and reported in Table S2 of ESI.†

Other useful information can be obtained by analyzing the differences between the experimental and the computed Stoke shifts.

Orange bars in the histogram reported in Fig. 3 show the Stoke shifts differences from the experimental values obtained using the maximum bands of the computed absorption and emission vibronic spectra. These results and the information obtained from the spectra in terms of band-shape and band positions suggest that the MN15 exchange–correlation functional reproduces the experimental values slightly better than the other functionals considered in this study.

A deeper investigation of the spectra obtained from MN15 calculations shows that for the **mono-bdp** system the computed absorption spectra present a more intense peak at 588 nm and a less intense one at 543 nm against the experimental ones at 595 nm and 547 nm, respectively. The computed difference between the two peaks of ∼40 nm matches the experimental value. Similar results have been obtained for the emission spectra of **mono-bdp** with a major peak at 595 nm and a minor one at 650 nm, whereas the experimental spectrum shows the intense peak at 605 nm and a weaker one at 655 nm. Even in this case, the difference between peak positions is in agreement with the experimental one. For **bis-bdp** too, the agreement between computations and experiments is consistent: the computed MN15 absorption spectra show a more intense peak at 745 nm and a less intense one at 672 nm against the experimental ones at 729 nm and 659 nm.

The simulated MN15 emission spectrum is characterized by a most intense peak at about 755 nm and a less intense one at 850 nm while the corresponding experimental one presents a major peak at 751 nm with a shoulder in the tail at 820 nm.

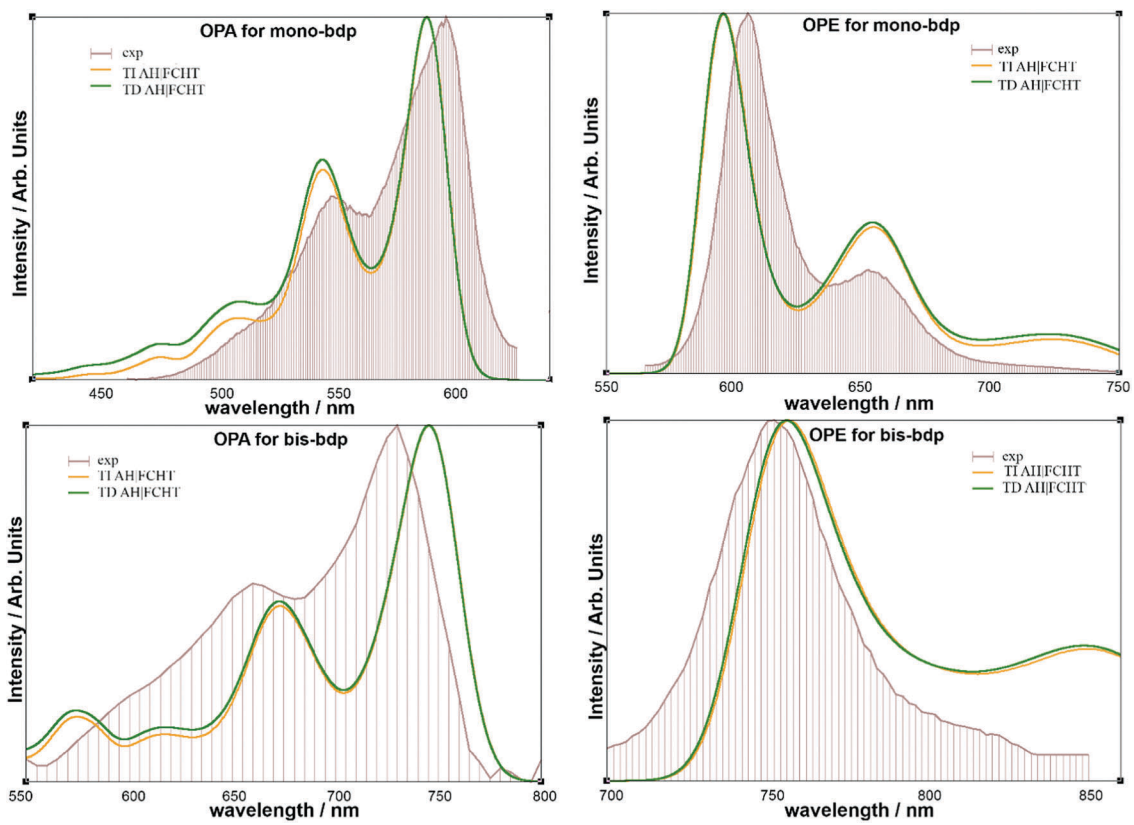

Fig. 4 Vibronic absorption and emission spectra of **mono-bdp** and **bis-bdp**, computed at the TD AH|FCHT and TI AH|FCHT levels, with the MN15 density functional and neglecting temperature effects, along with the experimental one recorded at 77 K in methanol. Gaussian distribution functions with HWHM = 250 cm^{-1} have been used to simulate the broadening.

In the histogram in Fig. 3, the blue bars indicate the Stoke shifts differences from the experimental values obtained using computed vertical excitation and emission energies with the NEQ-LR-PCM and EQ-SS-PCM approaches, respectively. While the red bars in the histogram are Stoke shifts differences from the experimental values obtained by using the computed vertical excitation and emission energies with the NEQ-SS-PCM and EQ-SS-PCM approaches, respectively.

While the former method slightly underestimates the Stoke shift almost systematically, the latter considerably overestimates it. The discrepancies observed between the three methods used to compute the Stokes shifts can be mainly rationalized considering that the methods diverge in the way by which the solvent effects are taken into account. In fact, in our vibronic calculations, the EQ-LR-PCM method is used both for the absorption and emission spectra. However, the vibronic effects, not accounted when the Stoke shift is computed using the vertical excitation energies, play an important role in reproducing such a property.

Numerical values are summarized in Table S3 of ESI† along with the experimental values.

Nature of the electronic transitions and vibronic contributions

Once we selected the most appropriate exchange–correlation functional (MN15) for the spectroscopic investigation of the styryl substituted BODIPY systems, we performed a deeper study of the nature of the electronic transitions, still with TD AH|FCHT as a reference. Our quantum mechanical calculations indicate that the first singlet excited state is due to a dipole-allowed π–π^* transition from the highest occupied molecular orbital (HOMO) to the lowest unoccupied molecular orbital (LUMO) shown in Fig. S2 of the ESI.†

For both molecules, the HOMOs are delocalized over the whole molecule whereas the LUMOs are mainly localized on the BODIPY core. The first electronic transition seems to have a partial charge transfer (CT) character, as indicated by the electron density change ($\Delta\rho_{S1-S0}$) reported at the bottom of Fig. S2 of the ESI.† To determine the spatial extent associated to the electronic transition and to better quantify its CT character, the CT distance (d_{CT}), the transferred charge (q_{CT}), the dipole (μ_{CT}), and the H and t indexes proposed by Ciofini and coworkers[67,68] have been computed and reported in Table 1. The q_{CT} parameter is a measure of the transferred charge, d_{CT} measures the distance between the center of mass (COM) of the atoms where the charge increases and the COM of the atoms where the charge decreases during the transition. μ_{CT} is the dipole moment associated with the charge transfer, the H index is a measure of the spread of the positive and negative charge variations in the donor and acceptor moieties whereas the t index, defined as the difference between the CT distance and the H index, measures the overlap between the electron-donating and electron-accepting regions. A negative value denotes an overlap between the two regions.

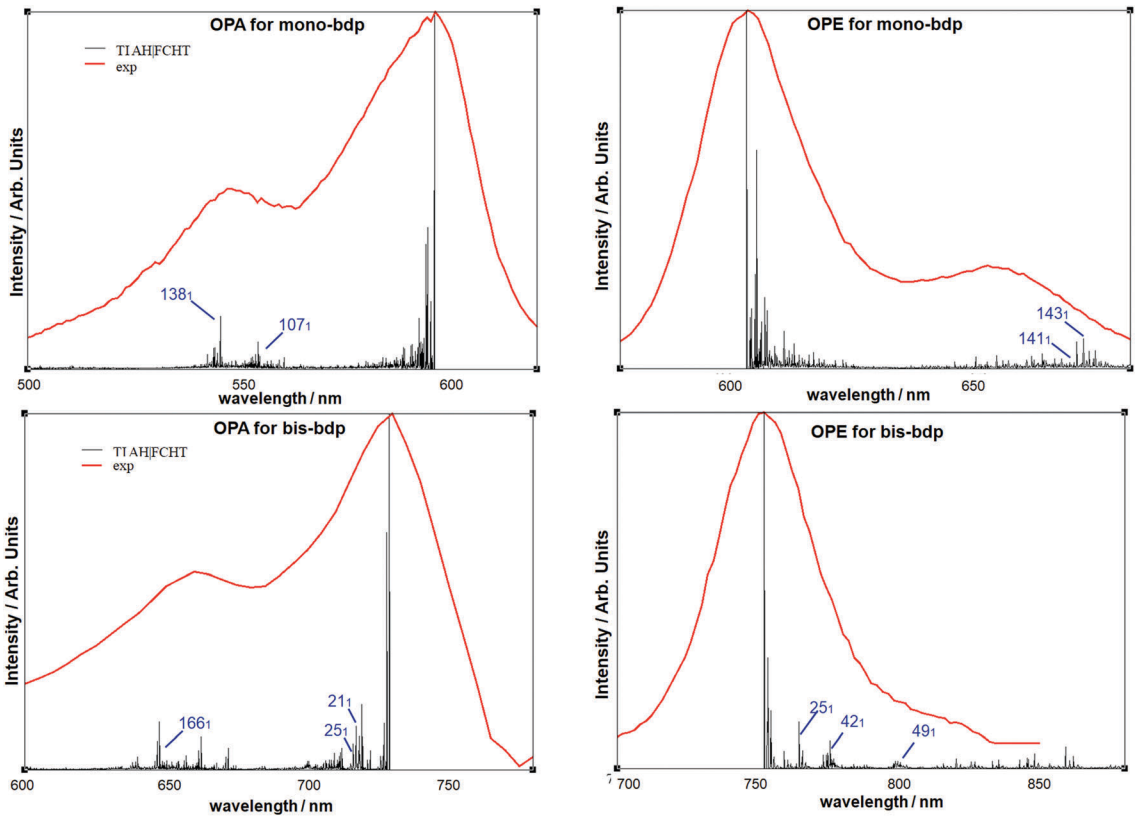

Fig. 5 Comparison between the experimental (red lines) and computed (blue histograms) absorption and emission vibronic spectra of **mono-bdp** and **bis-bdp** molecules. The theoretical spectra have been shifted in order to have the best agreement with the experimental ones.

The CT parameters for both molecules reveal that the transferred charge remains almost constant whereas the CT distance increases from 2.24 Å for **mono-bdp** to 3.21 Å for **bis-bdp**. This leads to a strong increment of the CT dipole and a separation of the electron-donating and electron-accepting regions. Therefore, the second styryl branch causes an enhancement of the CT character of the first excited state in BODIPY molecules, consistent with previous calculations.[40]

Comparison between vibronic models

The vibronic investigation described so far has been performed using the highest level of theory (*i.e.*, TD AH|FCHT). In this section, we have tested other, less expensive models to the study of the absorption and emission spectra of BODIPY systems, trying to evaluate also the reproducibility among methods.

In Fig. 4 the absorption and emission vibronic spectra of **mono-bdp** and **bis-bdp** computed at the MN15 level, neglecting temperature effects, using both TI and TD frameworks and Franck–Condon approximation with the Herzberg–Teller extension for the transition dipole moment are reported, along with the experimental spectra recorded at 77 K, in methanol.

To facilitate the comparison with experiments, a single broadening method has been used for all computed spectra (with half-widths at half-maximum of 250 cm^{-1}). Both TI AH|FCHT and TD AH|FCHT protocols reproduce nicely the vibronic structure with little shifts from the experimental band positions.

Some discrepancies found between the TI AH|FCHT and TD AH|FCHT methods are due to incomplete convergences from TI, linked to the intrinsic definition of this formalism.

The sum-over-states approach (TI method) can be used to analyze contributions of individual transitions to parts of the whole band-shape. Our computations, performed at the TI AH|FCHT level with the MN15 density functional, show that the 0–0 transition is the dominant one whereas the shoulders are composed of a blend of several vibrational states. The most important vibronic contributions with shifts from the 0–0 transition greater than 50 cm^{-1} are assigned in Fig. 5 and are due to fundamental bands (single-quantum excitations of one normal mode).

In particular, the shoulder in the absorption spectrum of **mono-bdp** is ascribed to the fundamental transition of mode 138 (1574 cm^{-1}) and 107 (1291 cm^{-1}). In the emission spectra of **mono-bdp**, the minor peak is given by the fundamental transitions of modes 141 and 143. Regarding the absorption spectrum of **bis-bdp**, the shoulder is ascribed to the fundamental transition of mode 166 (1614 cm^{-1}). Finally, the shoulder in the emission spectra of **bis-bdp** is attributed to the single-quantum excitations of normal modes 25, 42 and 49.

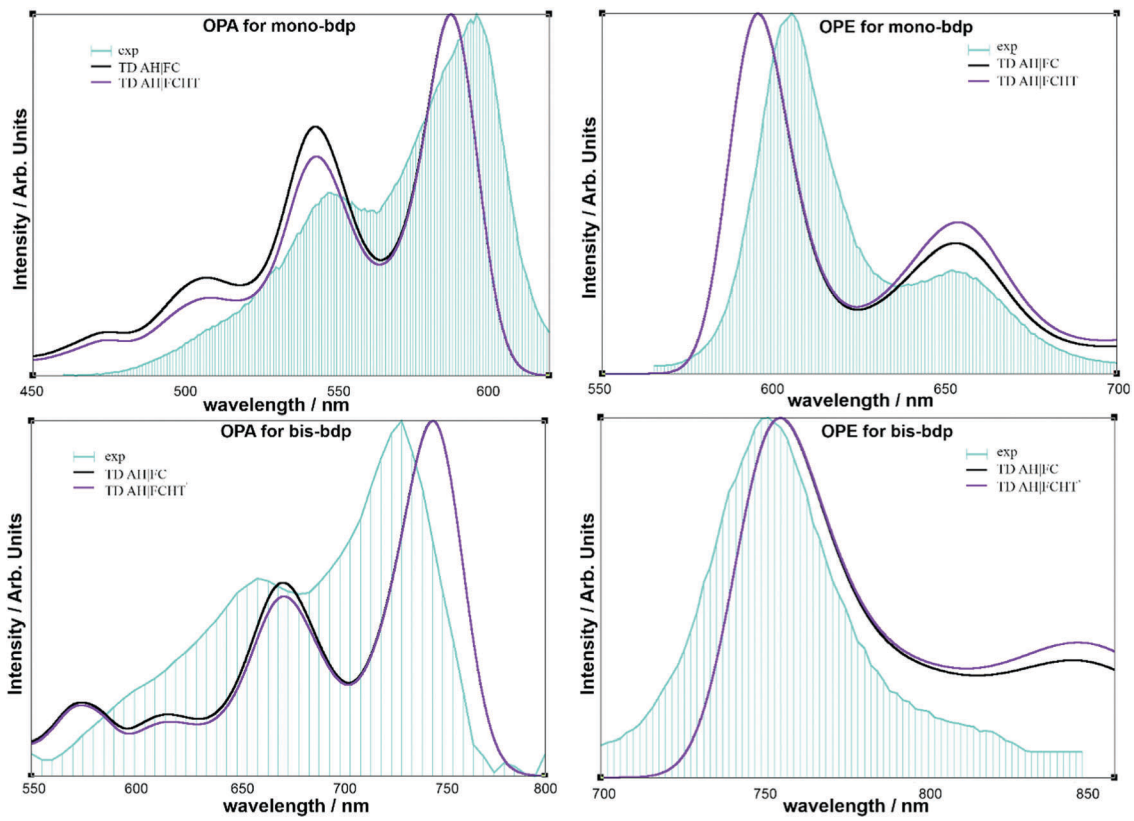

Fig. 6 Vibronic absorption and emission spectra of **mono-bdp** and **bis-bdp**, computed at the TD AH|FCHT and TD AH|FC levels, with the MN15 density functional and neglecting temperature effects, along with the experimental one recorded at 77 K in methanol. Gaussian distribution functions with HWHM = 250 cm^{-1} have been used to simulate the broadening.

The modes listed above are reported in Fig. S3 of the ESI† together with a representation of the corresponding vibrations. However, it must be kept in mind that all these normal modes involve the simultaneous oscillation of several atoms of the molecule and are thus extremely difficult to classify in terms of localized stretchings and bendings.

To investigate the effect of the Herzberg–Teller contributions, the vibronic absorption and emission spectra of **mono-bdp** and **bis-bdp** systems were computed at the TD AH|FCHT and TD AH|FC levels of theory, as reported in Fig. 6, with the experimental spectra recorded at 77 K in methanol as a reference.

As expected since the electronic transition is fully allowed, the spectra in Fig. 6 clearly show that there are no relevant differences between the FC and FCHT vibronic spectra of styryl substituted BODIPYs. In both cases, the band-shape is well reproduced and its position correct, and the relative heights of the major and minor peaks are almost in agreement with the experiments.

These comparisons between computed and experimental vibronic spectra show that all levels of theory considered give reproducible results: band shapes and positions are similar at all levels, and little improvement in terms of band shape has been found when including the Herzberg–Teller effect. This finding is particularly worthwhile if analytic first derivatives of the transition moment are not available and generating them numerically represent a significant increase of the computational cost or for the use of reduced-dimensionality schemes.

Table 2 Maximum band positions of the absorption and emission spectra computed at the TD AH|FC and TD AS|FC levels of theory and the corresponding Stoke shift values, together with the experimental data. All values are expressed in nm

	Absorption (nm)	Emission (nm)	Stoke shift (nm)
Mono-bdp			
Exp	596	605	9
TD AH|FC	587	595	8
TD AS|FC	575	582	7
Bis-bdp			
Exp	729	751	22
TD AH|FC	744	756	12
TD AS|FC	718	729	11

Next, the effect of mode mixing was investigated by comparing the adiabatic Hessian level of theory and its adiabatic shift approximation. The critical changes can be directly related to the fact that the approximated model (AS) ignores the mode mixing associated with the transition. The vibronic spectra reported in Fig. 7 show that for both styryl modified BODIPY systems, the TD AH|FC bands provide a better agreement with experiments, both in terms of band shape and position, than the TD AS|FC bands, confirming the importance of correctly accounting for the mode-mixing associated with the transition. The difference between TD AH|FC and TD AS|FC vibronic spectra is more obvious in terms of band position rather than

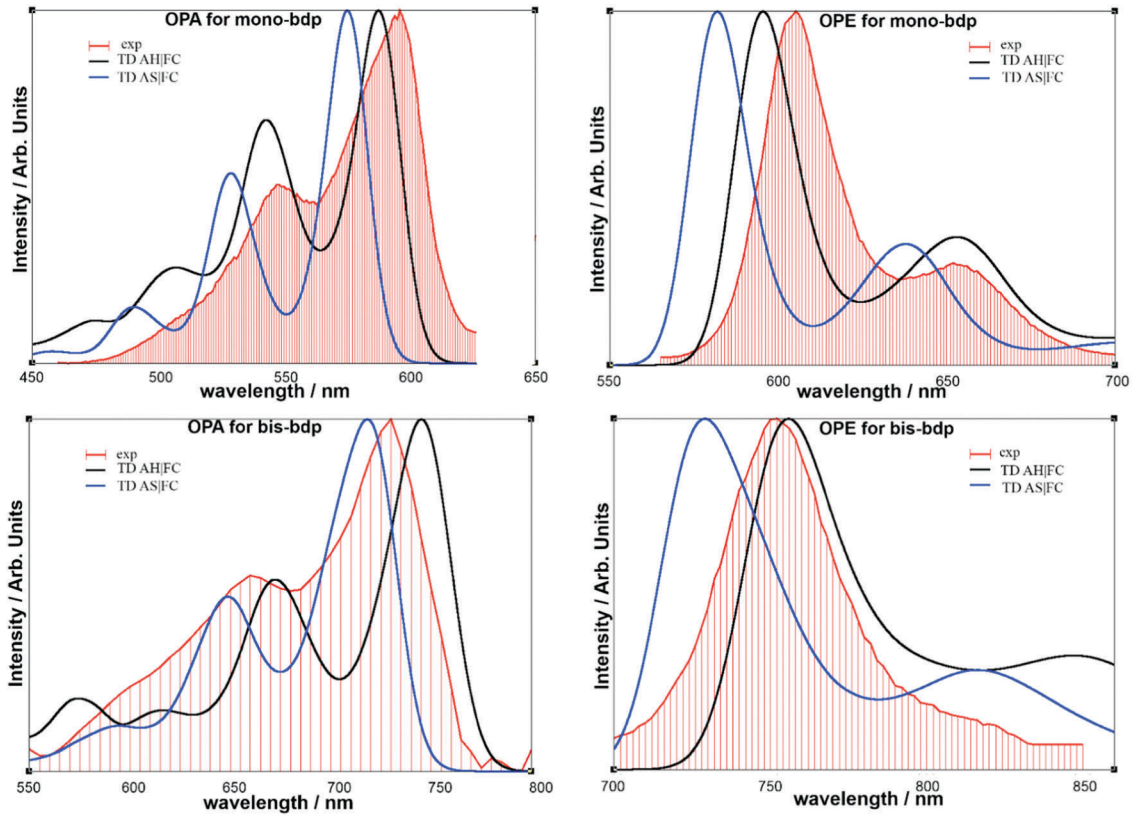

Fig. 7 Vibronic absorption and emission spectra of **mono-bdp** and **bis-bdp**, computed at the TD AH|FC and TD AS|FC levels, with the MN15 density functional. Gaussian distribution functions with HWHM = 250 cm^{-1} have been used to simulate the broadening.

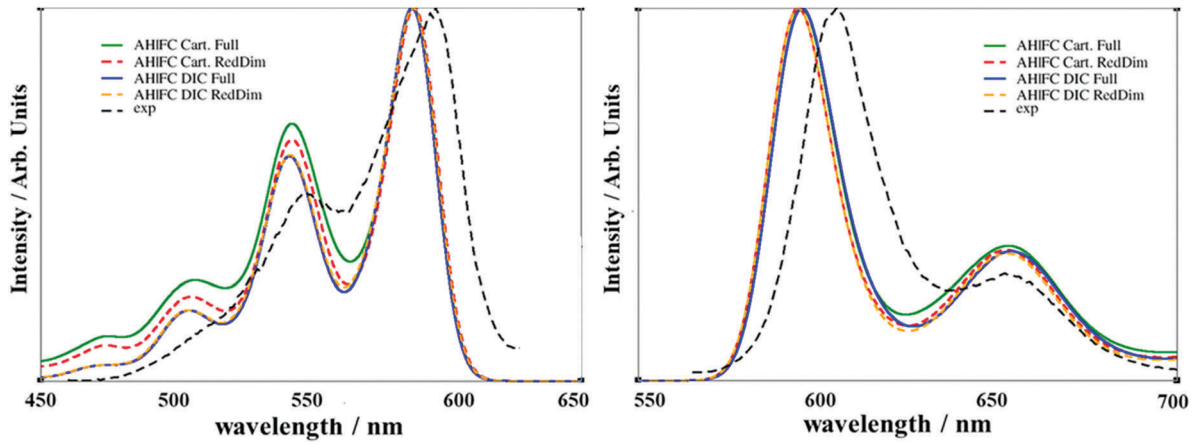

Fig. 8 OPA (left panel) and OPE (right panel) spectra of **mono-bdp** at the TD AH|FC level and T = 0 K, taking into account all normal modes (full, solid lines) or excluding low-energy ones (RedDim, dashed lines). Calculations were done with Cartesian (Cart.) and Internal (DIC) coordinates, using Gaussian distribution functions with half-widths at half-maximum of 250 cm^{-1} to simulate the broadening.

in terms of band shape. The difference in the former is due to the fact that the effect of the differences in ZPVE between the excited and ground states have been cancelled-out since changes in frequencies in the excited state are neglected with AS.

This evidence is also supported by the data reported in Table 2, where the maximum band values of the absorption and emission spectra computed using these two different levels of theory and their corresponding Stoke shift values are listed, together with the experimental data.

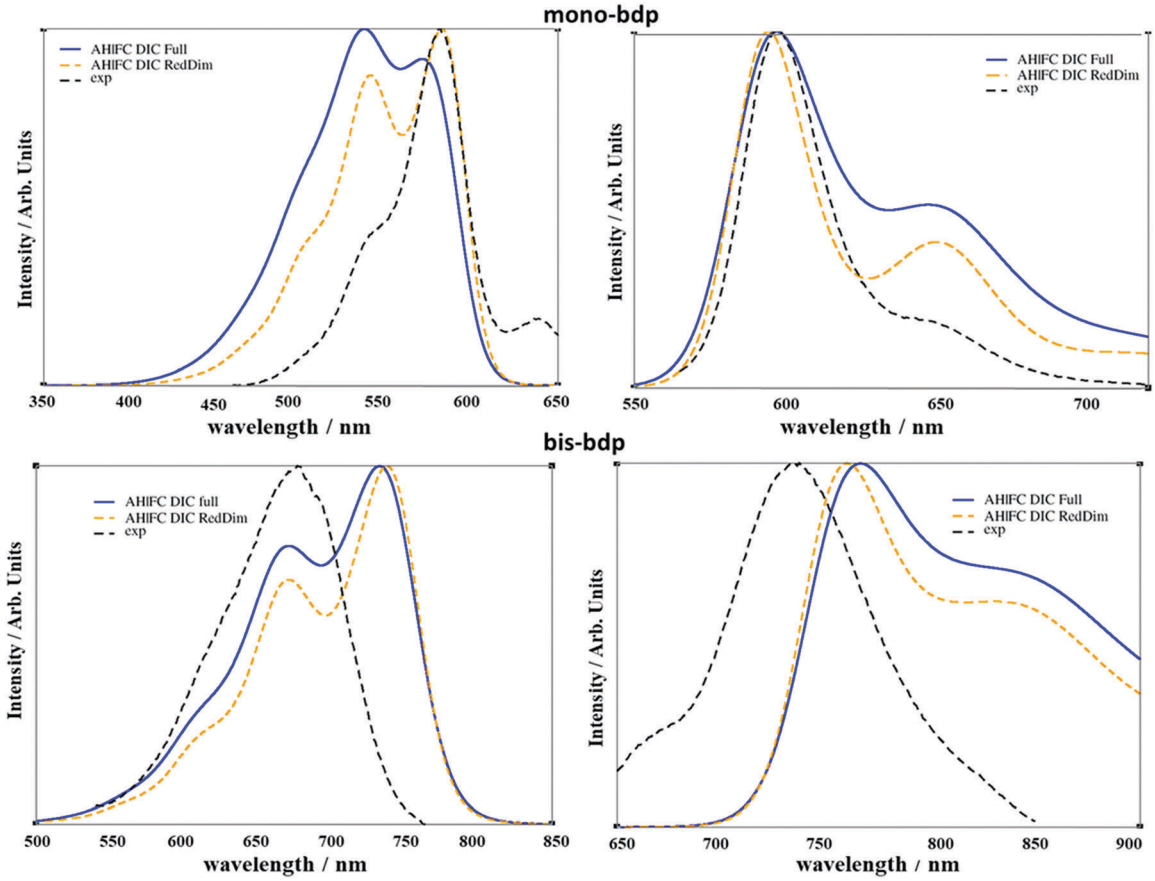

Fig. 9 Vibronic absorption and emission spectra of **mono-bdp** and **bis-bdp**, at room temperature, computed at the TD AH|FC level based on MN15 calculations, using the full and reduced-dimensionality definitions of the molecular systems. Gaussian distributions functions with half-widths at half-maximum of 250 cm^{-1} were used to simulate the broadening.

Temperature effects

Simulations of temperature effects on the full system give unsatisfactory results due to the presence of large amplitude motions (LAMs) in both initial and final states. These are poorly described at the harmonic level within the Franck–Condon framework and often give a small contribution to the overall band-shape. To overcome this issue, it is necessary to separate the system in two parts, which is done by dividing the Duschinsky into two square blocks; a small one with the modes to discard, and a large one with the modes correctly treated at the FC level. In order to avoid any unphysical description, the coupling between the two blocks, which can be estimated from the Duschinsky matrix, needs to be minimized. The overall iterative procedure followed here is described in ref. 64. The default coupling threshold of 10% was however too restrictive with respect to the size and flexibility of the BODIPYs and a higher threshold, set to 40% was used. An initial set of modes with wavenumbers below 50 cm^{-1} was automatically selected. These correspond to the first six modes for **mono-bdp** and eight for **bis-bdp**. In order to check the reliability of the reduced-dimensionality scheme, the OPA and OPE spectra of **mono-bdp** were computed at T = 0 K with the TD AH|FC scheme based both on the full and reduced Duschinsky matrices. The spectra are shown in Fig. 8. Some discrepancies can be observed in both spectra using the Cartesian-based normal coordinates between the complete and reduced systems, hinting at the presence of non-negligible couplings between the two blocks, which had been ignored in their construction. By switching to internal coordinates, using the non-redundant delocalized internal coordinates (DICs), an excellent match is obtained for the OPA spectrum, indicating that no significant coupling was ignored. The effect is less pronounced for OPE, where discrepancies still remain between the reduced and full system, albeit at a lesser degree than when using Cartesian coordinates. For consistency, the same set of normal modes was excluded for both OPA and OPE; however, an *ad hoc* treatment could be necessary to correct the slight discrepancies. The room temperature OPA and OPE spectra are displayed in Fig. 9, using internal coordinates for the simulations. For **mono-bdp**, a significant improvement in the description of the system can be noted after discarding the low-energy, large-amplitude motions, with the first band at 580 nm in the OPA spectrum correctly reproduced. Nevertheless, the second band at 540 nm still appears too intense, albeit not anymore as the strongest feature of the overall spectrum as shown in the full-dimensionality system. The remaining discrepancies could be due to other LAMs still present in the model system or the neglected impact of the discarded modes. For OPE, similar conclusions can be drawn, with the overall band-shape better reproduced with the reduced-dimensionality system, albeit in this case, the full treatment was better than for OPA. For **bis-bdp**, the results are less evident. While an improvement is observed in both spectra, it is of lesser extent. The most likely reason is that **bis-bdp** is more flexible than **mono-bdp** and the LAMs cannot be simply ignored but need to be treated either with explicit variational models, which would be too expensive for such systems, or through dynamic simulations.[69]

Conclusions

In this work, we show how several methods, adapted for semi-rigid molecules based on the Franck–Condon principle, can be used to study spectroscopic properties of BODIPY systems and to understand the influence of functional groups on their spectroscopic features, namely absorption and emission wavelengths and charge transfer.

To this end, the vibrationally resolved electronic spectra of two styryl substituted BODIPY molecules of technological interest were simulated, using both TI and TD formalisms, and compared with the available experimental data recorded in methanol.

As first step in this investigation of the styryl modified BODIPYs, several density functionals were benchmarked at the highest TD AH|FCHT level of theory, to select the most appropriate one. Similarly to previous investigations,[17,20,31] we have found that all benchmarked functionals have given good results in terms of band-shape but some of them presented huge discrepancies in terms of band position. Our computations have shown that the MN15 exchange–correlation functional, tested in this work for the first time, reproduces the experimental values slightly better than the other functionals considered.

Using this functional, a deeper analysis of the nature of the electronic transitions was performed and we have found that the first electronic transition seems to have a partial charge transfer (CT) character.

In addition, we tested how other levels of theory can be applied to the study of the optical properties of these two modified BODIPY systems, evaluating the reproducibility among methods.

It has been found that all levels of theory considered give reproducible results for the investigated systems: band positions and shapes are similar at all levels and little improvements have been found in terms of band-shape with the inclusion of the Herzberg–Teller term. Inclusion of temperature effects on such large, flexible systems proved challenging for our vibronic models. However, carefully tailoring the theoretical model with a suitable set of coordinates, it is possible to obtain a qualitative agreement with experimental results. Nevertheless, significant discrepancies remain, which may require new, *ad hoc* treatments in order to get a completely accurate picture.

Finally, this analysis represents a first, preliminary step for further investigations of systems involving other, more complex two-dimensional spectroscopic techniques.

Conflicts of interest

There are no conflicts to declare.

Acknowledgements

This work is financially supported by the ''Ministero dell'Istruzione, dell'Università e della Ricerca'' MIUR through the PRIN2015 project (Prot. no. 2015XBZ5YA) entitled: toward quantum photovoltaic: ultrafast energy and charge transport in hybrid nanomaterials. The high performance computer facilities of the SMART Laboratory (http://smart.sns.it) are acknowledged for providing computer resources.We thank Dr Massimiliano Cordaro (University of Messina) for providing the samples of the investigated molecules.

Notes and references

1 A. C. Benniston and G. Copley, Lighting the way ahead with boron dipyrromethene (Bodipy) dyes, *Phys. Chem. Chem. Phys.*, 2009, **11**, 4124–4131.
2 N. Boens, V. Leen and W. Dehaen, Fluorescent indicators based on BODIPY, *Chem. Soc. Rev.*, 2012, **41**, 1130–1172.
3 M. Benstead, G. H. Mehl and R. W. Boyle, 4,4′-Difluoro-4-bora-3a,4a-diaza-s-indacenes (BODIPYs) as components of novel light active materials, *Tetrahedron*, 2011, **67**, 3573–3601.
4 A. Kamkaew, S. H. Lim, H. B. Lee, L. V. Kiew, L. Y. Chung and K. Burgess, BODIPY Dyes In Photodynamic Therapy, *Chem. Soc. Rev.*, 2013, **42**, 77–88.
5 C. Adamo and D. Jacquemin, The calculations of excited-state properties with Time-Dependent Density Functional Theory, *Chem. Soc. Rev.*, 2013, **42**, 845–856.
6 P. Cimino, A. Pedone, E. Stendardo and V. Barone, Interplay of stereo-electronic, environmental, and dynamical effects in determining the EPR parameters of aromatic spin-probes: INDCO as a test case, *Phys. Chem. Chem. Phys.*, 2010, **12**, 3741–3746.
7 A. J. Cohen, P. Mori-Sánchez and W. Yang, Challenges for Density Functional Theory, *Chem. Rev.*, 2012, **112**, 289–320.
8 A. Dreuw and M. Head-Gordon, Single-Reference ab Initio Methods for the Calculation of Excited States of Large Molecules, *Chem. Rev.*, 2005, **105**, 4009–4037.
9 D. Jacquemin, B. Mennucci and C. Adamo, Excited-state calculations with TD-DFT: from benchmarks to simulations in complex environments, *Phys. Chem. Chem. Phys.*, 2011, **13**, 16987–16998.
10 B. Mennucci, Modeling environment effects on spectroscopies through QM/classical models, *Phys. Chem. Chem. Phys.*, 2013, **15**, 6583–6594.
11 A. Pedone, M. Biczysko and V. Barone, Environmental Effects in Computational Spectroscopy: Accuracy and Interpretation, *ChemPhysChem*, 2010, **11**, 1812–1832.
12 A. Pedone, G. Prampolini, S. Monti and V. Barone, Absorption and emission spectra of fluorescent silica nanoparticles from TD-DFT/MM/PCM calculations, *Phys. Chem. Chem. Phys.*, 2011, **13**, 16689–16697.
13 A. Pedone, G. Prampolini, S. Monti and V. Barone, Realistic Modeling of Fluorescent Dye-Doped Silica Nanoparticles: A Step Toward the Understanding of their Enhanced Photophysical Properties, *Chem. Mater.*, 2011, **23**, 5016–5023.
14 D. Presti, F. Labat, A. Pedone, M. J. Frisch, H. P. Hratchian, I. Ciofini, M. C. Menziani and C. Adamo, Computational Protocol for Modeling Thermochromic Molecular Crystals: Salicylidene Aniline As a Case Study, *J. Chem. Theory Comput.*, 2014, **10**, 5577–5585.
15 E. Runge and E. K. U. Gross, Density-Functional Theory for Time-Dependent Systems, *Phys. Rev. Lett.*, 1984, **52**, 997–1000.
16 B. Le Guennic and D. Jacquemin, Taking Up the Cyanine Challenge with Quantum Tools, *Acc. Chem. Res.*, 2015, **48**, 530–537.
17 S. Chibani, A. D. Laurent, B. Le Guennic and D. Jacquemin, Improving the Accuracy of Excited-State Simulations of BODIPY and Aza-BODIPY Dyes with a Joint SOS-CIS(D) and TD-DFT Approach, *J. Chem. Theory Comput.*, 2014, **10**, 4574–4582.
18 S. Chibani, B. Le Guennic, A. Charaf-Eddin, O. Maury, C. Andraud and D. Jacquemin, On the Computation of Adiabatic Energies in Aza-Boron-Dipyrromethene Dyes, *J. Chem. Theory Comput.*, 2012, **8**, 3303–3313.
19 A. D. Laurent and D. Jacquemin, TD-DFT benchmarks: a review, *Int. J. Quantum Chem.*, 2013, **113**, 2019–2039.
20 B. L. Guennic, O. Maury and D. Jacquemin, Aza-boron-dipyrromethene dyes: TD-DFT benchmarks, spectral analysis and design of original near-IR structures, *Phys. Chem. Chem. Phys.*, 2011, **14**, 157–164.
21 D. Jacquemin, E. A. Perpète, G. Scalmani, M. J. Frisch, R. Kobayashi and C. Adamo, Assessment of the efficiency of long-range corrected functionals for some properties of large compounds, *J. Chem. Phys.*, 2007, **126**, 144105.
22 M. R. Momeni and A. Brown, Why Do TD-DFT Excitation Energies of BODIPY/Aza-BODIPY Families Largely Deviate from Experiment? Answers from Electron Correlated and Multireference Methods, *J. Chem. Theory Comput.*, 2015, **11**, 2619–2632.
23 M. Filatov, Description of electron transfer in the ground and excited states of organic donor–acceptor systems by single-reference and multi-reference density functional methods, *J. Chem. Phys.*, 2014, **141**, 124123.
24 A. D. Quartarolo, N. Russo and E. Sicilia, Structures and electronic absorption spectra of a recently synthesised class of photodynamic therapy agents, *Chem. Weinh. Bergstr. Ger.*, 2006, **12**, 6797–6803.
25 D. Jacquemin, A. Planchat, C. Adamo and B. Mennucci, TD-DFT Assessment of Functionals for Optical 0–0 Transitions in Solvated Dyes, *J. Chem. Theory Comput.*, 2012, **8**, 2359–2372.
26 D. Jacquemin, V. Wathelet, E. A. Perpète and C. Adamo, Extensive TD-DFT Benchmark: Singlet-Excited States of Organic Molecules, *J. Chem. Theory Comput.*, 2009, **5**, 2420–2435.
27 R. Improta, V. Barone and F. Santoro, Ab Initio Calculations of Absorption Spectra of Large Molecules in Solution: Coumarin C153, *Angew. Chem., Int. Ed.*, 2007, **46**, 405–408.
28 A. Pedone, J. Bloino and V. Barone, Role of Host–Guest Interactions in Tuning the Optical Properties of Coumarin Derivatives Incorporated in MCM-41: A TD-DFT Investigation, *J. Phys. Chem. C*, 2012, **116**, 17807–17818.
29 F. Santoro, R. Improta, A. Lami, J. Bloino and V. Barone, Effective method to compute Franck-Condon integrals for

optical spectra of large molecules in solution, *J. Chem. Phys.*, 2007, **126**, 084509.

30 F. Muniz-Miranda, A. Pedone, G. Battistelli, M. Montalti, J. Bloino and V. Barone, Benchmarking TD-DFT against Vibrationally Resolved Absorption Spectra at Room Temperature: 7-Aminocoumarins as Test Cases, *J. Chem. Theory Comput.*, 2015, **11**, 5371–5384.

31 S. Chibani, B. L. Guennic, A. Charaf-Eddin, A. D. Laurent and D. Jacquemin, Revisiting the optical signatures of BODIPY with ab initio tools, *Chem. Sci.*, 2013, **4**, 1950–1963.

32 F. Egidi, D. B. Williams-Young, A. Baiardi, J. Bloino, G. Scalmani, M. J. Frisch, X. Li and V. Barone, Effective Inclusion of Mechanical and Electrical Anharmonicity in Excited Electronic States: VPT2-TDDFT Route, *J. Chem. Theory Comput.*, 2017, **13**, 2789–2803.

33 J. Liu and W. Liang, Analytical Hessian of electronic excited states in time-dependent density functional theory with Tamm-Dancoff approximation, *J. Chem. Phys.*, 2011, **135**, 014113.

34 J. Liu and W. Liang, Analytical approach for the excited-state Hessian in time-dependent density functional theory: formalism, implementation, and performance, *J. Chem. Phys.*, 2011, **135**, 184111.

35 A. Baiardi, J. Bloino and V. Barone, General Time Dependent Approach to Vibronic Spectroscopy Including Franck–Condon, Herzberg–Teller, and Duschinsky Effects, *J. Chem. Theory Comput.*, 2013, **9**, 4097–4115.

36 V. Barone, *Computational Strategies for Spectroscopy: From Small Molecules to Nano Systems*, John Wiley & Sons, 2011.

37 J. Bloino, A. Baiardi and M. Biczysko, Aiming at an accurate prediction of vibrational and electronic spectra for medium-to-large molecules: an overview, *Int. J. Quantum Chem.*, 2016, **116**, 1543–1574.

38 V. Barone, J. Bloino, M. Biczysko and F. Santoro, Fully Integrated Approach to Compute Vibrationally Resolved Optical Spectra: From Small Molecules to Macrosystems, *J. Chem. Theory Comput.*, 2009, **5**, 540–554.

39 J. Bloino, M. Biczysko, F. Santoro and V. Barone, General Approach to Compute Vibrationally Resolved One-Photon Electronic Spectra, *J. Chem. Theory Comput.*, 2010, **6**, 1256–1274.

40 L. Bolzonello, A. Polo, A. Volpato, E. Meneghin, M. Cordaro, M. Trapani, M. Fortino, A. Pedone, M. A. Castriciano and E. Collini, Two-Dimensional Electronic Spectroscopy Reveals Dynamics and Mechanisms of Solvent-Driven Inertial Relaxation in Polar BODIPY Dyes, *J. Phys. Chem. Lett.*, 2018, **9**, 1079–1085.

41 M. Dierksen and S. Grimme, Density functional calculations of the vibronic structure of electronic absorption spectra, *J. Chem. Phys.*, 2004, **120**, 3544–3554.

42 D. Jacquemin, E. Brémond, A. Planchat, I. Ciofini and C. Adamo, TD-DFT Vibronic Couplings in Anthraquinones: From Basis Set and Functional Benchmarks to Applications for Industrial Dyes, *J. Chem. Theory Comput.*, 2011, **7**, 1882–1892.

43 E. Stendardo, F. Avila, F. Santoro and R. Improta, Vibrationally resolved absorption and emission spectra of dithiophene in the gas phase and in solution by first-principle quantum mechanical calculations, *J. Chem. Theory Comput.*, 2012, **8**, 4483–4493.

44 J. Bloino, M. Biczysko, O. Crescenzi and V. Barone, Integrated computational approach to vibrationally resolved electronic spectra: anisole as a test case, *J. Chem. Phys.*, 2008, **128**, 244105.

45 M. de Groot and W. J. Buma, Vibronic spectra of the lower excited singlet states of styrene: a time dependent density functional theory study, *Chem. Phys. Lett.*, 2007, **435**, 224–229.

46 G. Herzberg and E. Teller, Schwingungsstruktur der Elektronenübergänge bei mehratomigen Molekülen, *Z. Für Phys. Chem.*, 1933, **21B**, 410–446.

47 I. Pugliesi, N. M. Tonge, K. E. Hornsby, M. C. R. Cockett and M. J. Watkins, An examination of structural characteristics of phenylacetylene by vibronic and rovibronic simulations of ab initio data, *Phys. Chem. Chem. Phys.*, 2007, **9**, 5436–5445.

48 A. Hazra, H. H. Chang and M. Nooijen, First principles simulation of the UV absorption spectrum of ethylene using the vertical Franck-Condon approach, *J. Chem. Phys.*, 2004, **121**, 2125–2136.

49 N. M. Tonge, E. C. MacMahon, I. Pugliesi and M. C. R. Cockett, The weak hydrogen bond in the fluorobenzene-ammonia van der Waals complex: insights into the effects of electron withdrawing substituents on pi versus in-plane bonding, *J. Chem. Phys.*, 2007, **126**, 154319.

50 M. J. Frisch, G. W. Trucks, H. B. Schlegel, G. E. Scuseria, M. A. Robb, J. R. Cheeseman, G. Scalmani, V. Barone, A. Petersson, H. Nakatsuji, X. Li, M. Caricato, A. V. Marenich, J. Bloino, B. G. Janesko, R. Gomperts, B. Mennucci, H. P. Hratchian, J. V. Ortiz, A. F. Izmaylov, J. L. Sonnenberg, D. Williams-Young, F. Ding, F. Lipparini, F. Egidi, J. Goings, B. Peng, A. Petrone, T. Henderson, D. Ranasinghe, V. G. Zakrzewski, J. Gao, N. Rega, G. Zheng, W. Liang, M. Hada, M. Ehara, K. Toyota, R. Fukuda, J. Hasegawa, M. Ishida, T. Nakajima, Y. Honda, O. Kitao, H. Nakai, T. Vreven, K. Throssell, J. A. Montgomery, Jr., J. E. Peralta, F. Ogliaro, M. Bearpark, J. J. Heyd, E. Brothers, K. N. Kudin, V. N. Staroverov, T. A. Keith, R. Kobayashi, J. Normand, K. Raghavachari, A. Rendell, J. C. Burant, S. S. Iyengar, J. Tomasi, M. Cossi, J. M. Millam, M. Klene, C. Adamo, R. Cammi, J. W. Ochterski, R. L. Martin, K. Morokuma, Ö. Farkas, J. B. Foresman and D. J. Fox, *Gaussian 16, Revision B.01*, Gaussian, Inc., Wallingford, CT, 2016.

51 A. D. Becke, Density-functional thermochemistry. III. The role of exact exchange, *J. Chem. Phys.*, 1993, **98**, 5648–5652.

52 C. Adamo and V. Barone, Toward reliable density functional methods without adjustable parameters: the PBE0 model, *J. Chem. Phys.*, 1999, **110**, 6158–6170.

53 T. Yanai, D. P. Tew and N. C. Handy, A new hybrid exchange-correlation functional using the Coulomb-attenuating method (CAM-B3LYP), *Chem. Phys. Lett.*, 2004, **1–3**, 51–57.

54 J.-D. Chai and M. Head-Gordon, Systematic optimization of long-range corrected hybrid density functionals, *J. Chem. Phys.*, 2008, **128**, 084106.

55 Y. Zhao and D. G. Truhlar, Density functional for spectroscopy: no long-range self-interaction error, good performance for Rydberg and charge-transfer states, and better performance on average than B3LYP for ground states, *J. Phys. Chem. A*, 2006, **110**, 13126–13130.
56 H. S. Yu, X. He, S. L. Li and D. G. Truhlar, MN15: a Kohn–Sham global-hybrid exchange–correlation density functional with broad accuracy for multi-reference and single-reference systems and noncovalent interactions, *Chem. Sci.*, 2016, **7**, 5032–5051.
57 S. Grimme, Semiempirical GGA-type density functional constructed with a long-range dispersion correction, *J. Comput. Chem.*, 2006, **27**, 1787–1799.
58 S. Grimme, Semiempirical hybrid density functional with perturbative second-order correlation, *J. Chem. Phys.*, 2006, **124**, 034108.
59 J.-D. Chai and M. Head-Gordon, Long-range corrected hybrid density functionals with damped atom–atom dispersion corrections, *Phys. Chem. Chem. Phys.*, 2008, **10**, 6615–6620.
60 E. Cancès, B. Mennucci and J. Tomasi, A new integral equation formalism for the polarizable continuum model: theoretical background and applications to isotropic and anisotropic dielectrics, *J. Chem. Phys.*, 1997, **107**, 3032–3041.
61 R. Improta, G. Scalmani, M. J. Frisch and V. Barone, Toward effective and reliable fluorescence energies in solution by a new state specific polarizable continuum model time dependent density functional theory approach, *J. Chem. Phys.*, 2007, **127**, 074504.
62 R. Improta, V. Barone, G. Scalmani and M. J. Frisch, A state-specific polarizable continuum model time dependent density functional theory method for excited state calculations in solution, *J. Chem. Phys.*, 2006, **125**, 054103.
63 A. Pedone, Role of Solvent on Charge Transfer in 7-Aminocoumarin Dyes: New Hints from TD-CAM-B3LYP and State Specific PCM Calculations, *J. Chem. Theory Comput.*, 2013, **9**, 4087–4096.
64 A. Baiardi, J. Bloino and V. Barone, General formulation of vibronic spectroscopy in internal coordinates, *J. Chem. Phys.*, 2016, **144**, 084114.
65 D. Wang, Y. Shiraishi and T. Hirai, A distyryl BODIPY derivative as a fluorescent probe for selective detection of chromium(III), *Tetrahedron Lett.*, 2010, **51**, 2545–2549.
66 D. Licari, A. Baiardi, M. Biczysko, F. Egidi, C. Latouche and V. Barone, Implementation of a graphical user interface for the virtual multifrequency spectrometer: the VMS-Draw tool, *J. Comput. Chem.*, 2015, **36**, 321–334.
67 C. Adamo, T. Le Bahers, M. Savarese, L. Wilbraham, G. García, R. Fukuda, M. Ehara, N. Rega and I. Ciofini, Exploring excited states using time dependent density functional theory and density-based indexes, *Coord. Chem. Rev.*, 2015, **304–305**, 166–178.
68 T. Le Bahers, C. Adamo and I. Ciofini, A Qualitative Index of Spatial Extent in Charge-Transfer Excitations, *J. Chem. Theory Comput.*, 2011, **7**, 2498–2506.
69 A. Patoz, T. Begušić and J. Vaníček, On-the-Fly Ab Initio Semiclassical Evaluation of Absorption Spectra of Polyatomic Molecules beyond the Condon Approximation, *J. Phys. Chem. Lett.*, 2018, **9**, 2367–2372.

